IEEE Access
Multidisciplinary | Rapid Review | Open Access Journal

Received December 29, 2021, accepted January 14, 2022, date of publication January 18, 2022, date of current version January 26, 2022.

Digital Object Identifier 10.1109/ACCESS.2022.3144231

Wideband Four-Port Single-Patch Antenna Based on the Quasi-$TM_{1/2,1/2}$ Mode for 5G MIMO Access-Point Application

KIN-LU WONG[1], (Fellow, IEEE), XIAN-QI YE[1], (Student Member, IEEE), AND WEI-YU LI[2], (Member, IEEE)

[1]Department of Electrical Engineering, National Sun Yat-sen University, Kaohsiung 80424, Taiwan
[2]Information and Communications Research Laboratories, Industrial Technology Research Institute, Hsinchu 31057, Taiwan

Corresponding author: Kin-Lu Wong (wongkl@mail.nsysu.edu.tw)

This work was supported by the Ministry of Science and Technology, Taiwan, under Grant MOST 110-2224-E-110-001 and Grant MOST 108-2221-E-110-005.

ABSTRACT A wideband four-port single-patch antenna for fifth-generation (5G) MIMO access-point application in 3.3-5.0 GHz (41% centered at 4.15 GHz) is presented. The antenna uses a simple square patch of size 42 mm x 42 mm (0.58λ x 0.58λ at 4.15 GHz) mounted 10 mm above a ground plane. To generate four isolated waves in a wide band for MIMO application, the square patch is short-circuited to the ground plane using four simple L-shape metal walls to form four resonant quadrants for the quasi-$TM_{1/2,1/2}$ mode excitation. Each resonant quadrant is excited using a slot-coupled probe feed to have dual-resonance behavior with good impedance matching over a wide band. It is obtained that the single-patch antenna can generate four isolated waves in 3.3-5.0 GHz with impedance matching better than −10 dB, port isolation >15 dB, antenna efficiency >80%, and envelope correlation coefficients <0.03. Details of the proposed antenna are presented. An extended design for enhanced port isolation of the proposed antenna is also studied.

INDEX TERMS Four-port single-patch antennas, MIMO antennas, 5G access-point antennas, $TM_{1/2,1/2}$ modes.

I. INTRODUCTION

For fifth-generation (5G) 4 x 4 multi-input-multi-output (MIMO) operation, both the terminal device and access point require multiple antennas to be embedded therein. For this purpose, compact four-antenna elements capable of generating four isolated waves are attractive for the terminal-device and access-point applications [1]–[7]. For the terminal device, the four-antenna elements backed by a ground plane and having a low-profile structure of about 1 mm to be especially suitable for application in the back cover of the terminal device have been reported [2]–[4], which leads to compact integration of the MIMO antenna and the terminal device.

For the access point, it has been shown that the four-antenna elements can lead to large size reduction for the MIMO antenna array [5]. For example, the antenna array formed by using the four-antenna element, such as the four-port single-patch antenna [5], [6], can have a much smaller array size (less than about one half) as compared to a conventional antenna array based on using the traditional two-port dual-polarized antenna element.

In order to achieve the four-port single-patch antenna generating four isolated waves over a wide band, the excitation of multiple (five) resonant modes for each port on a single slotted square patch mounted about 15.7 mm (0.38λ at 7.25 GHz) above a ground plane has been demonstrated to cover 6.0-8.5 GHz (bandwidth 34.5% centered at 7.25 GHz) [5]. The outer dimensions of the multimode square patch are 0.85λ x 0.85λ at the center frequency. Recently, a four-port annular-ring patch antenna generating four isolated waves in 3.3-5.0 GHz (bandwidth 41% centered at 4.15 GHz) for the MIMO access-point application has also been shown [7]. The annular-ring patch has an outer diameter of 56 mm, about 0.77λ at 4.15 GHz. Four isolated waves related to the monopolar patch antenna (MPA) mode [8], [9] are generated with very low envelope correlation coefficients (ECCs less than 0.05) over the wide band [7].

The associate editor coordinating the review of this manuscript and approving it for publication was Adao Silva.

TABLE 1. Comparison of reported wideband four-port single-patch antennas with four isolated waves for MIMO access-point application.

Ref.	[5], [6]	[7]	This work
Antenna height	15.7mm (0.38λ@ 7.25GHz)	10mm (0.14λ@ 4.15GHz)	10mm (0.14λ@ 4.15GHz)
Patch size	0.85λ x 0.85λ	0.77λ x 0.77λ	0.58λ x 0.58λ
Operating bandwidth	6.0-8.5GHz (34.5%)	3.3-5.0GHz (41%)	3.3-4.5GHz (41%)
Antenna efficiency	> 70%	> 80%	> 80%
ECC	< 0.01	< 0.05	< 0.03
Antenna modes	Multiple (five)-modes excited for each port	Monopolar patch antenna (MPA) mode excited for each port	Quasi-$TM_{1/2,1/2}$ mode excited for each port
External feed network	Required	No	No
Structure complexity	Complex	Complex	Simple

However, it is noted that, in order to achieve four-port operation with good port isolation for the wideband MIMO access-point application, the outer dimension of the reported four-port antenna is still as large as 0.85λ in [5], [6] or 0.77λ in [7]. The four-antenna elements with more compact in patch size and much simpler in antenna structure are still demanding for MIMO access-point antenna application.

In this study, a new wideband four-port single-patch antenna for 5G MIMO access-point application in 3.3-5.0 GHz (41% centered at 4.15 GHz) is presented. To achieve a compact single-patch structure yet supporting four isolated waves, a simple square patch is formed into four quadrants by using four simple L-shape metal walls to short-circuit the square patch to the ground plane. In this case, each cavity quadrant between the square patch and ground plane can support the quasi-$TM_{1/2,1/2}$ mode excitation. With the slot-coupled feed, the excited quasi-$TM_{1/2,1/2}$ mode can have dual-resonance behavior to achieve a wide band of larger than 40%. Additionally, the four excited quasi-$TM_{1/2,1/2}$ modes for the four resonant quadrants of the square-patch antenna show good isolation in the wide band.

A comparison of the proposed antenna (this work) and the reported wideband four-port single-patch antennas [5]–[7] for MIMO access-point application is also summarized in Table 1. Note that the length of the square patch in the proposed design is only 42 mm (0.58λ at 4.15 GHz), which is relatively much smaller as compared to the reported wideband four-port single-patch antennas in [5]–[7]. In addition, in the wide band of 3.3.-5.0 GHz, the proposed antenna generates four isolated waves with antenna efficiency >80%, good port isolation >15 dB, and envelope correlation coefficients (ECCs) <0.03. With a relatively smaller patch size, the proposed antenna also generates four isolated waves over a wide band.

Different resonant modes are also excited in [5]–[7] and in the proposed antenna for each port to achieve the wideband operation. In [5], [6], multiple (five) resonant modes are required for each port to achieve the wideband operation

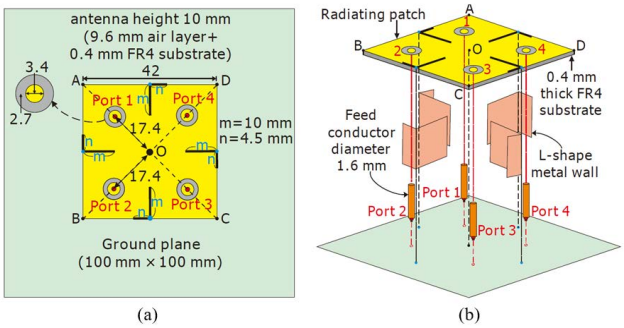

FIGURE 1. Geometry of the proposed four-port single-patch MIMO antenna. (a) Top view. (b) Exploded view.

and the external feed network is also required, which makes its antenna structure complex. In [7], the monopolar patch antenna (MPA) mode for each port is excited. Its patch structure is also relatively complex and has a larger size than the proposed antenna.

The proposed antenna requires no external feed network, which is needed in [5], [6]. Additionally, the use of a simple square patch with the quasi-$TM_{1/2,1/2}$ mode excitation leads to a simpler antenna structure and also a smaller patch size than those used in [5]–[7]. Details of the proposed antenna and the experimental results are presented. To further enhance the port isolation of the four ports in the proposed antenna, an extended design is also studied.

II. FOUR-PORT SINGLE-PATCH ANTENNA

Fig. 1 shows the proposed four-port single-patch MIMO antenna. The antenna dimensions are selected to cover 3.3-5.0 GHz for 5G MIMO access-point application. The single patch is a simple square patch of length 42 mm (0.58λ at 4.15 GHz) and is mounted 10 mm (0.14λ at 4.15 GHz) above a ground plane of size 100 mm x 100 mm. The length of the ground plane is selected to be larger than one wavelength of the lower-edge frequency (3.3 GHz) in the wide band, so that the possible contribution of the ground plane to the antenna's resonant modes in the study can be reduced to be minimum. Additionally, the large ground plane can also result in a higher antenna gain.

To support the quasi-$TM_{1/2,1/2}$ mode, the square patch is short-circuited to the ground plane by using four L-shape metal walls (0.2 mm thick copper plate) with an inner metal wall of length 10 mm (m) along the patch's center line and an edge metal wall of length 4.5 mm (n) along the patch's side edge. Four inner metal walls configure the cavity region between the square patch and ground plane into four cavity quadrants. For each cavity quadrant, there are two shorting metal walls of length m along two orthogonal directions, making it capable of supporting the quarter-wavelength resonance in two orthogonal directions. That is, the excitation of the $TM_{1/2,1/2}$ mode can be supported.

Note that, by considering that the resonant cavity has a height of 10 mm (0.14λ at 4.15 GHz), not like the conventional cavity model applied for the patch antenna with a

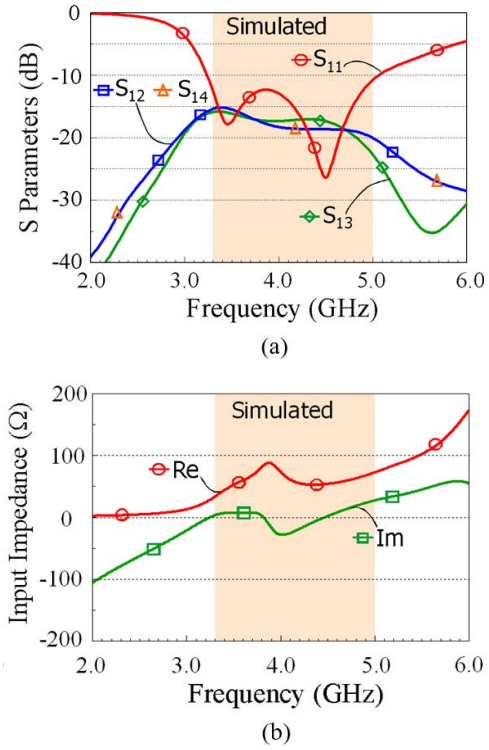

FIGURE 2. Simulated (a) *S* parameters and (b) input impedance of Port 1 in the proposed design.

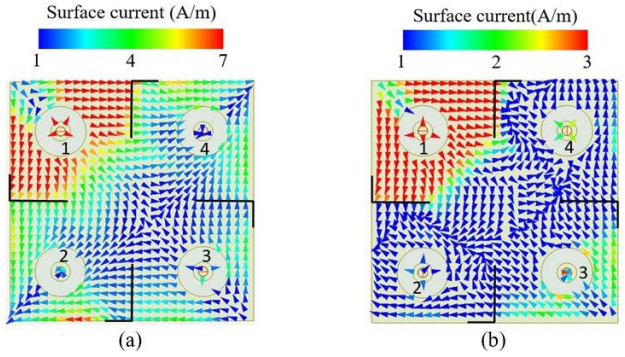

FIGURE 3. Simulated vector surface current distributions of Port 1 (other ports terminated to 50 Ω) in the proposed design. (a) 3.45 GHz. (b) 4.5 GHz.

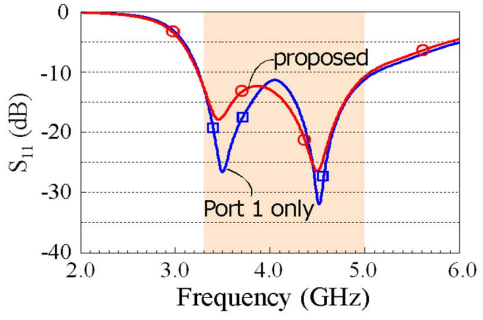

FIGURE 4. Simulated S_{11} of Port 1 in the proposed design and the case of Port 1 only (Ports 2-4 in Fig. 1 not present).

very low profile [10], [11], the quasi-TM$_{1/2,1/2}$ mode is used here. As for applying the edge metal wall of length n along

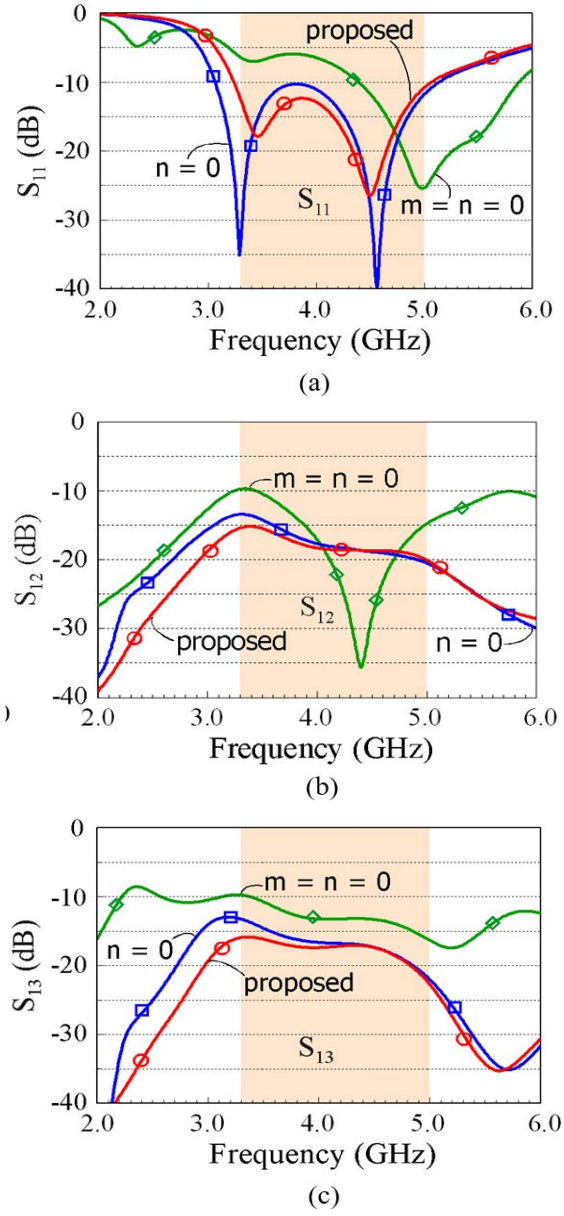

FIGURE 5. Simulated *S* parameters of Port 1 in the proposed design, the case without the edge metal walls ($n = 0$), and the case without the L-shape metal walls ($m = n = 0$). (a) S_{11}. (b) S_{12} (= S_{14}). (c) S_{13}.

the patch's side edge, it enhances the isolation between the excited quasi-TM$_{1/2,1/2}$ modes in the desired wide band.

In order to excite the quasi-TM$_{1/2,1/2}$ mode, the ring slot-coupled probe feed is placed along the diagonal lines of the square patch. The ring slot has an inner diameter of 3.4 mm and a gap of 2.7 mm to compensate for the contributed inductance of the 10 mm long probe conductor. Owing to the slot-coupled probe feed, the dual-resonance behavior [12] of the excited quasi-TM$_{1/2,1/2}$ mode is obtained, which leads to a wide band of 3.3-5.0 GHz.

Also, for easy implementation of the feed structure, the square patch is printed on a thin FR4 substrate (thickness 0.4 mm, relative permittivity 4.4, loss tangent 0.024)

spaced 9.6 mm to the ground plane to keep an antenna height of 10 mm. In this case, the effective relative permittivity of the antenna substrate is close to unity. Wider bandwidth and higher antenna efficiency for the four cavity quadrants operated like quarter-wavelength patches can be obtained [11].

By applying the simulation tool of the high-frequency structure simulator (HFSS) [13], the selected dimensions of the proposed design are shown in Fig. 1. The simulated S parameters and input impedance of Port 1 are shown in Fig. 2. Owing to the symmetric structure of the proposed design, the results of Ports 2-4 are same as those of Port 1 and are not shown for brevity. The colored region in the figure indicates the desired band of 3.3-5.0 GHz, in which the reflection coefficient S_{11} is less than -10 dB and the transmission coefficients (S_{12}, S_{13}, S_{14}) are all less than -15 dB [see Fig. 2(a)].

Also, because of the symmetric structure, both the S_{12} and S_{14} are the same. Due to the two resonant modes at about 3.45 and 4.5 GHz seen in the S_{11} curve, the proposed design achieves a wide operating band. The two resonant modes occur at frequencies close to the zero imaginary (Im) part of the input impedance seen in Fig. 2(b). Smooth variation of the input impedance in the desired wide band is also obtained, which is owing to the use of the ring slot-coupled probe feed. This makes the two resonant modes with good impedance matching in 3.3-5.0 GHz.

Note that when the square patch in the proposed antenna is printed on a thicker FR4 substrate (for example, 0.8 mm thick FR4 substrate spaced 9.2 mm above the ground plane) instead of the 0.4 mm thick FR4 substrate spaced 9.6 mm above the ground plane in the study, the coupling ring-slot gap of the probe feed in the square patch can be increased from 2.7 mm here to be 3.6 mm to achieve similar impedance matching. Both cases are of the same 10 mm thick antenna substrate. In this case, the reflection coefficient of the excited two resonant modes in 3.3-5.0 GHz can also be less than -10 dB.

This is mainly because, by adjusting the ring-slot gap, similar coupling of the ring slot-coupled probe feed for both cases of using 0.4 mm and 0.8 mm thick FR4 substrates can be obtained. However, in order to make the effective relative permittivity of the antenna substrate to be close to unity so as to achieve wider bandwidth and higher antenna efficiency [11] for the proposed design, the FR4 substrate of a smaller thickness is used here.

To further analyze the two resonant modes, Fig. 3 shows the simulated vector surface current distributions of Port 1 at 3.45 and 4.5 GHz in the proposed design. It is seen that the surface current distributions of Port 1 at the two frequencies are similar and are mainly confined within the same quadrant. The current distributions indicate that the quarter-wavelength resonance along each one of the two orthogonal patch edges is excited at both 3.45 and 4.5 GHz. That is, the quasi-$TM_{1/2,1/2}$ mode with dual resonance in 3.3-5.0 GHz is excited in the cavity quadrant formed by two nearby L-shape metal walls.

Additional results of the simulated S_{11} of Port 1 in the proposed design and the case of Port 1 only (Ports 2-4 in Fig. 1 not present) are shown in Fig. 4. It is seen that similar S_{11} curves with dual resonance are observed. This indicates that when Ports 2-4 are added in the other three quadrants, small effects on the Port 1 excitation are obtained. This suggests that simply owing to the four L-shape metal walls, the four cavity quadrants in the proposed design can support the quasi-$TM_{1/2,1/2}$ mode excitation with small coupling to each other in a wide band.

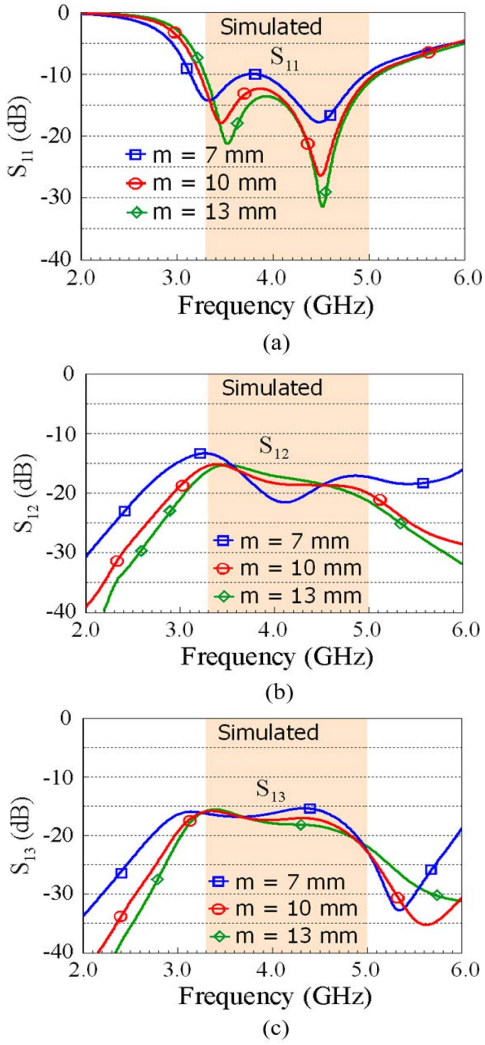

FIGURE 6. Simulated S parameters of Port 1 in the proposed design with various lengths of the inner metal walls. (a) S_{11}. (b) S_{12} (=S_{14}) (c) S_{13}.

Effects of the inner and edge metal walls are also studied. Fig. 5 shows the simulated S parameters of Port 1 in the proposed design, the case without the edge metal walls ($n = 0$), and the case without the L-shape metal walls ($m = n = 0$). The S_{11}, S_{12} ($= S_{14}$), and S_{13} are shown in Fig. 5(a), (b), and (c), respectively. When both the inner and edge metal walls are not present ($m = n = 0$), poor impedance matching and isolation of Ports 1-4 in 3.3-5.0 GHz are seen. With the presence of the inner metal wall only ($m = 10$ mm, $n = 0$ in Fig. 1), both impedance matching and isolation of Ports 1-4 are greatly improved.

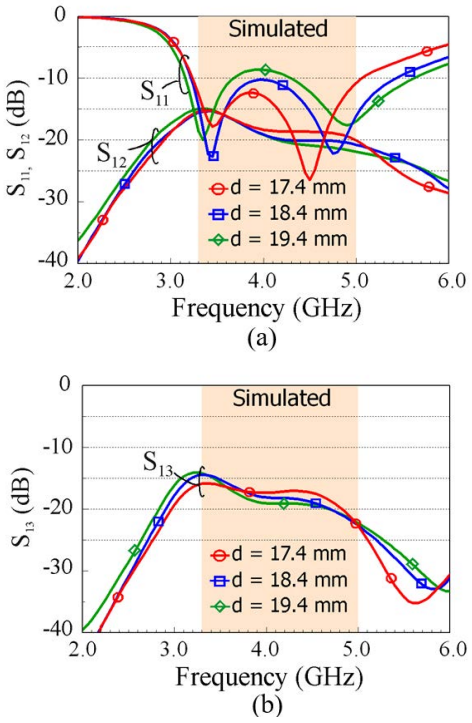

FIGURE 7. Simulated *S* parameters of Port 1 as a function of the feed position (*d*) to the patch center. (a) S_{11}, S_{12} (= S_{14}). (b) S_{13}.

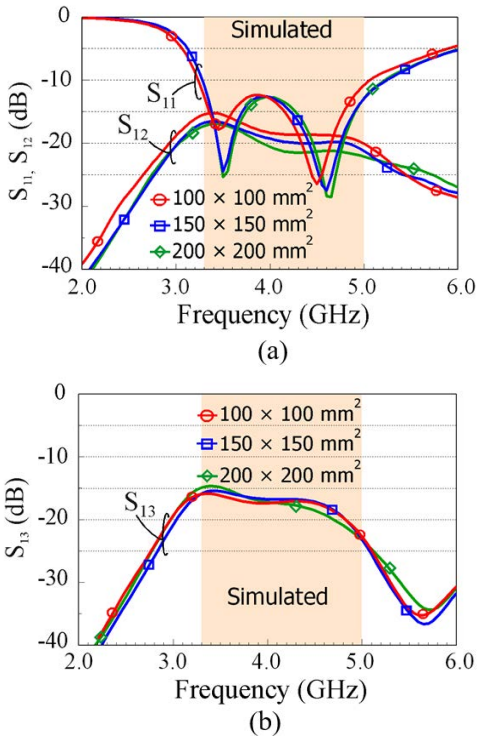

FIGURE 8. Simulated *S* parameters of Port 1 as a function of the ground plane size. (a) S_{11}, S_{12} (= S_{14}). (b) S_{13}.

When the edge metal wall of length n is also added (the proposed case), the isolation can be further enhanced. It is obtained that the S_{12} and S_{13} are lower than -15 dB in 3.3-5.0 GHz, with the S_{11} kept to be lower than -10 dB. Based on the results, it is suggested that the inner metal walls of length m mainly form the required cavity quadrants for Ports 1-4 to excite the quasi-TM$_{1/2,1/2}$ mode with dual-resonance behavior to cover a wide operating band. For the edge metal walls of length n, it can achieve enhanced isolation of Ports 1-4.

To finely adjust the dual-resonance behavior of the quasi-TM$_{1/2,1/2}$ mode, the length of the inner metal walls can be adjusted. Fig. 6 shows the simulated *S* parameters of Port 1 in the proposed design with various lengths of the inner metal walls. The length of the edge metal walls is fixed to be 4.5 mm as in Fig. 1. Results of the S_{11}, S_{12} (= S_{14}), and S_{13} for the length m varied from 7 mm to 13 mm are shown. For m = 10 mm and 13 mm, the dual resonance of the quasi-TM$_{1/2,1/2}$ mode is seen to have better impedance matching than that for m = 7 mm in the desired 3.3-5.0 GHz [see the S_{11} in Fig. 6(a)].

In addition, around the lower and upper edges of 3.3-5.0 GHz, the S_{11} is lower for m = 10 mm than for m = 13 mm. Also, as seen in Fig. 6(b) and (c), the S_{12} and S_{13} around 3.3 GHz are both lower than -15 dB for m = 10 mm and 13 mm. From the results in Fig. 6, the length m in the proposed design is selected to be 10 mm (about one quarter of the patch length 42 mm) as in Fig. 1.

Furthermore, the effects of the feed position (d) to the patch center and the ground plane size in the proposed antenna are analyzed. Fig. 7 shows the simulated *S* parameters of Port 1 for the feed position varied from 17.4 mm to 19.4 mm along the diagonal line to the patch center. Other dimensions are fixed as shown in Fig. 1. The results indicate that the S_{11} can be adjusted by varying the feed position. On the other hand, relatively small effects on the S_{12} (= S_{14}) and S_{13} are seen.

Fig. 8 shows the simulated *S* parameters of Port 1 for the ground plane size varied from 100 x 100 mm^2 to 200 x 200 mm^2. Other dimensions are also fixed as shown in Fig. 1. Small variations on the S_{11}, S_{12} (= S_{14}), and S_{13} are observed. The results confirm that the ground plane selected as 100 x 100 mm^2 in the study does not contribute to the antenna's resonant modes.

III. EXPERIMENTAL RESULTS AND DISCUSSION

The proposed antenna was fabricated as shown in Fig. 9. Note that the probe pins of Ports 2 and 4 are behind the L-shaped shorting walls in the side-view photo seeing from the direction of Port 1. Also, since Port 3 is in the opposite side of Port 1, the probe pin of Port 3 is behind that of Port 1. All the probe pins use copper posts of diameter 1.6 mm.

The measured reflection coefficients of Ports 1-4 are shown in Fig. 10(a), and the measured transmission coefficients of Port 1 to Ports 2-4 are shown in Fig. 10(b). The measured data generally agree with the simulated results of Port 1 shown in the figure. Note that, owing to the symmetric structure of the proposed antenna, the simulated results of Ports 2-4 are same as that of Port 1. The measured

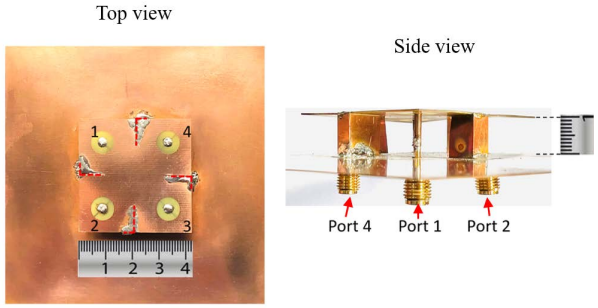

FIGURE 9. Photos of the top and side views of the fabricated prototype.

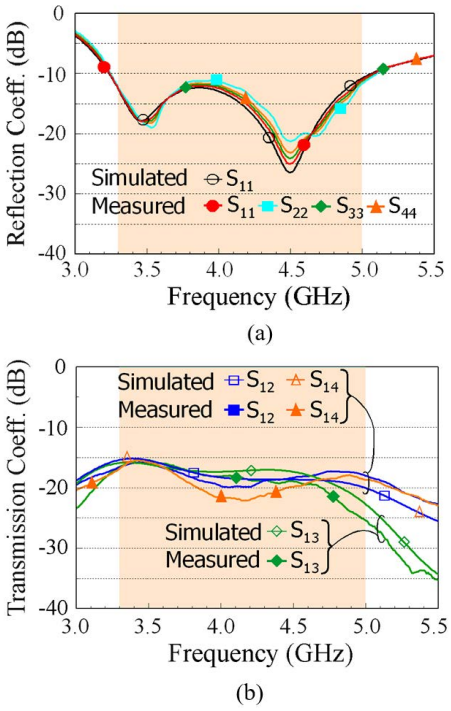

FIGURE 10. Measured (a) reflection coefficients and (b) transmission coefficients; Simulated S parameters of Port 1 are shown for comparison.

reflection coefficients of Ports 1-4 are lower than −10 dB in 3.3-5.0 GHz and the measured transmission coefficients are lower than −15 dB. The port isolation of the four ports is larger than 15 dB in the proposed 4-port patch antenna using a simple and compact square patch.

Fig. 11(a) and (b) show the measured antenna efficiency and antenna gain of Ports 1-4. The simulated results of Port 1 are shown in the figure for comparison. Fair agreement between the measured and simulated results is seen. The measured antenna efficiency is better than 80% and the measured antenna gain is about 6.1-7.5 dBi in 3.3-5.0 GHz.

The measured and simulated normalized radiation patterns of Port 1 at 3.45 and 4.5 GHz are plotted in Fig. 12. The radiation patterns in the two vertical planes (*x-z* and *y-z* planes) are shown. Fair agreement of the measured and simulated patterns is observed. It is seen that the radiation patterns with comparable E_θ and E_φ components are similar at the two frequencies. The obtained results are reasonable,

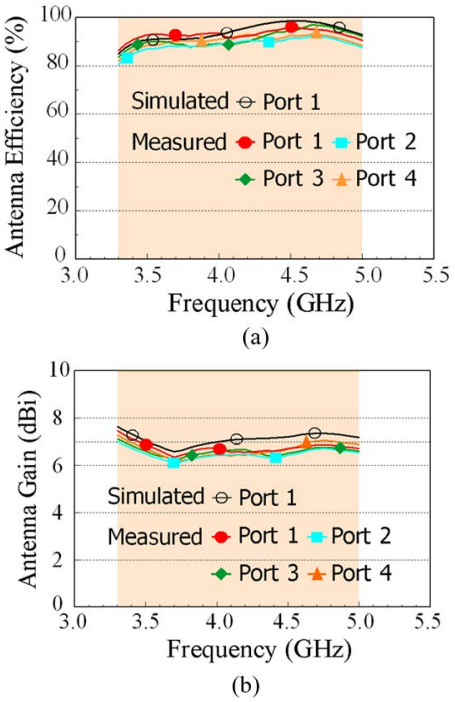

FIGURE 11. Measured (a) antenna efficiency and (a) antenna gain of Ports 1-4 in the fabricated prototype; Simulated results of Port 1 are shown for comparison.

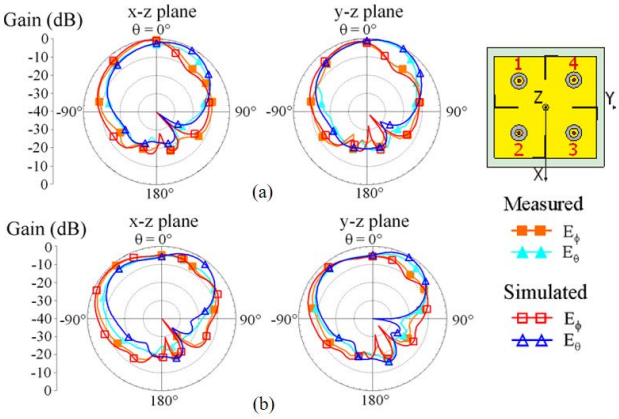

FIGURE 12. Measured and simulated normalized radiation patterns of Port 1. (a) 3.45 GHz. (b) 4.5 GHz.

since the $TM_{1/2,1/2}$ mode with dual resonance at 3.45 and 4.5 GHz is excited for the proposed antenna as discussed in Section II. For the $TM_{1/2,1/2}$ mode excitation, the same quarter-wavelength resonance in two orthogonal directions is supported. This agrees with the results of comparable E_θ and E_φ components seen in the radiation patterns. This radiation characteristic can be advantageous in achieving rich multi-path propagation for MIMO operation, especially in indoor MIMO propagation environment.

The simulated total active reflection coefficient (TARC) [14], [15] for the proposed antenna is also shown in Fig. 13. The TARC values are obtained by assuming that Ports 1-4 are all excited with same amplitude and phase for transmitting four synchronized MIMO signals in the HFSS

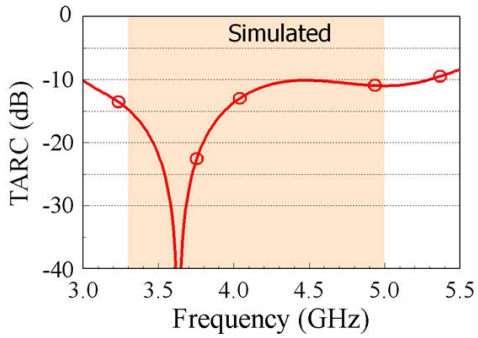

FIGURE 13. Simulated total active reflection coefficient (TARC) for the proposed antenna.

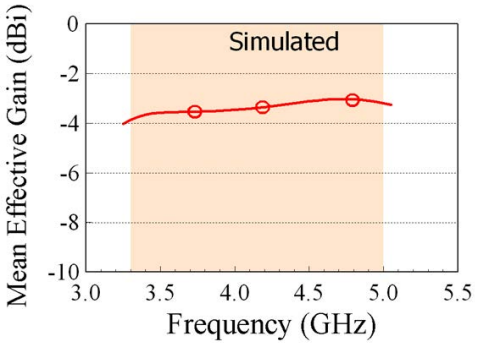

FIGURE 14. Simulated mean effective gain (MEG) of Port 1 in the proposed antenna.

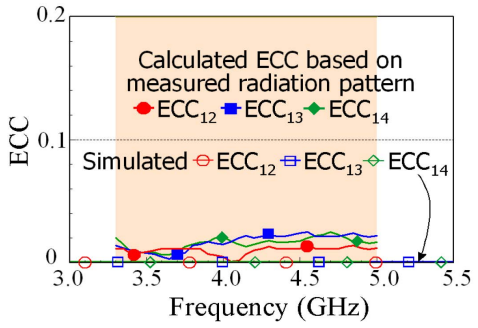

FIGURE 15. Calculated ECCs based on the measured radiation patterns; the HFSS simulated results are shown for comparison.

simulation [13]. The results show that the TARC values are less than −10 dB in 3.3-5.0 GHz. Also note that when the phases between the four ports are varied, there will be some variations on the TARC values.

In Fig. 14, the simulated mean effective gain (MEG) [14] of Port 1 in the proposed antenna is demonstrated. The isotropic uniform incident wave condition is assumed. In this case, owing to the symmetric structure of the four ports in the proposed antenna, the simulated MEG results of Ports 1-4 are the same. Therefore, only the result of Port 1 is shown in the figure. It is seen that the variations of the MEG of Port 1 are small (less than 1 dBi) in 3.3-5.0 GHz.

The calculated ECC based on the measured radiation patterns [14], [16] is presented in Fig. 15. The result between the radiating waves generated by Ports 1 and 2 is indicated

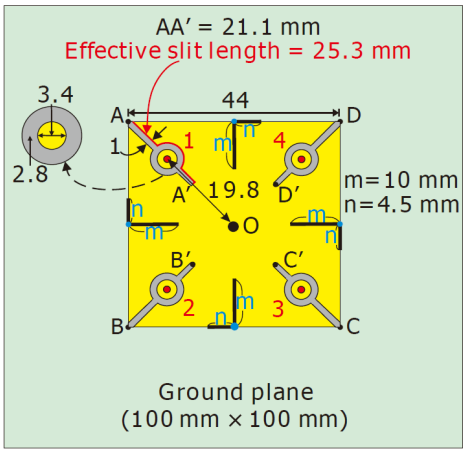

FIGURE 16. Four decoupling linear slits embedded along the diagonal line of the square patch in the proposed antenna (extended design). The antenna dimensions not given in the figure are same as in Fig. 1.

as ECC$_{12}$. The corresponding result between Ports 1 and 3 (Ports 1 and 4) is indicated as ECC$_{13}$ (ECC$_{14}$) in the figure. For comparison, the HFSS simulated ECC is also shown, which is very low (lower than 0.01). Very low measured ECCs (<0.03) are also obtained. The results suggest that the four radiating waves generated by Ports 1-4 can be considered to be isolated to each other. This characteristic is good for MIMO applications.

IV. STUDY ON ENHANCED PORT ISOLATION

The port isolation of the four ports in the proposed antenna in Fig. 1 is larger than 15 dB in the wide band of 3.3-5.0 GHz. A study on further enhancing the port isolation is also conducted. Fig. 16 shows an extended design of the proposed antenna by embedding four decoupling linear slits along the diagonal lines of the square patch. Each decoupling linear slit has an opening at the patch corner and also integrates with the ring-slot coupled feed for each port in the square patch.

The integrated linear slit and ring slot together have an effective slit length of 25.3 mm, about 0.22λ or close to one quarter-wavelength at 2.6 GHz. In this case, a band-notching characteristic for the transmission coefficients at around 2.6 GHz, outside the desired operating band, is obtained. This can lead to decreased port isolation in the operating band, with small effects on the impedance matching inside the desired operating band.

Also, the linear slits are embedded along the patch's diagonal lines, which are parallel to the excited surface currents of the quasi-TM$_{1/2,1/2}$ mode in the proposed antenna (see Fig. 3). Small effects on the antenna's resonant mode excitation are therefore expected. However, the embedded four decoupling linear slits still slightly increase the lower-edge frequency of the antenna's operating band. To compensate for this effect, the patch length is slightly increased from 42 mm in Fig. 1 to 44 mm in the extended design. The position of the ring-slot coupled feed is finely adjusted from 17.4 mm in Fig. 1 to be at 19.8 mm to the patch center. The coupling

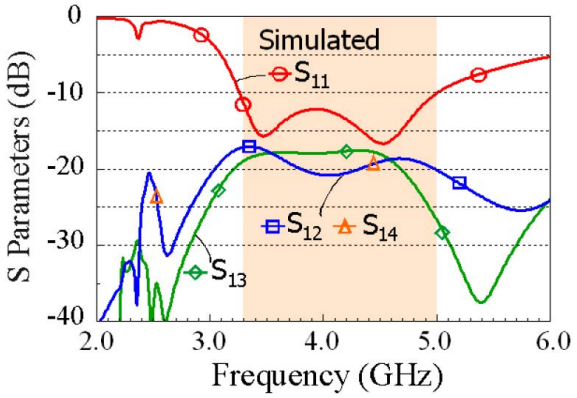

FIGURE 17. Simulated *S* parameters of Port 1 in the extended design. Results of Ports 2-4 are same as that of Port 1.

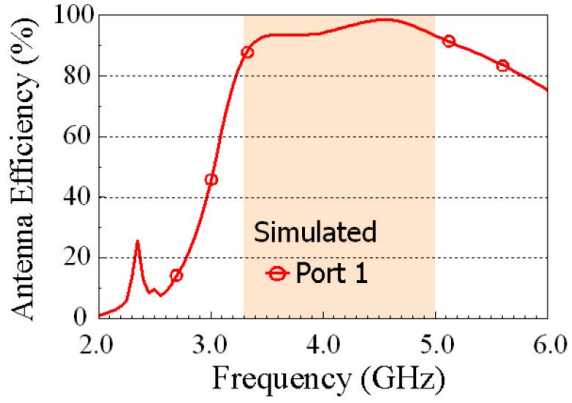

FIGURE 18. Simulated antenna efficiency of Port 1 in the extended design. Results of Ports 2-4 are same as that of Port 1.

ring-slot gap is adjusted to be 2.8 mm (2.7 mm in Fig. 1). Other antenna dimensions are same as given in Fig. 1 (the proposed antenna).

The simulated S parameters of Port 1 in the extended design are shown in Fig. 17. It is seen that, in the desired operating band of 3.3-5.0 GHz, the reflection coefficients are less than -10 dB. The transmission coefficients of S_{12} ($= S_{14}$) and S_{13} of Port 1 to Ports 2-4 are all lower than -17 dB over the wide band. The enhanced port isolation in the extended design as compared to the proposed antenna is related to the band-notching behavior seen in the transmission coefficients at about 2.6 GHz (see the dips in the S_{12} and S_{13} curves in the figure), which causes a decrease in the S_{12} and S_{13} in the operating band. The minimum S_{12} reaches -21 dB around 4 GHz and the minimum S_{13} is about -26 dB at 5.0 GHz. The minimum S_{12} and S_{13} are also lower than those in the proposed antenna [see Fig. 17 vs. Fig. 2(a)].

The simulated antenna efficiency (mismatching loss included) of Port 1 in the extended design is shown in Fig. 18. The antenna efficiency is larger than 83% in 3.3-5.0 GHz, similar to that in the proposed antenna [see Fig. 18 vs. Fig. 9(a)]. That is, the four ports in the extended design shows similar antenna performance as those in the proposed antenna, with better port isolation over the wide band of 3.3-5.0 GHz.

V. CONCLUSION

A four-port square-patch antenna generating four isolated waves in a wide band of 3.3-5.0 GHz for 5G MIMO access-point application has been presented. The proposed antenna has a compact single-patch structure to generate four isolated waves for the MIMO application. By applying four L-shape metal walls between the square patch and ground plane, four cavity quadrants can be formed to support the excitation of four dual-resonance quasi-TM$_{1/2,1/2}$ modes with good impedance matching and good port isolation in 3.3-5.0 GHz. Operating principle of the proposed antenna has been addressed, and experimental results have been shown to validate the simulation study. An extended design to achieve enhanced port isolation of the four ports is also demonstrated.

REFERENCES

[1] K.-L. Wong, "5G/B5G multi-gbps antennas for user terminals and their throughput verification," in *Proc. IEEE Asia–Pacific Microw. Conf. (APMC)*, Hong Kong, Dec. 2020, pp. 366–368.

[2] D. Q. Liu, H. J. Luo, M. Zhang, H. L. Wen, B. Wang, and J. Wang, "An extremely low-profile wideband MIMO antenna for 5G smartphones," *IEEE Trans. Antennas Propag.*, vol. 67, no. 9, pp. 5772–5780, Sep. 2019.

[3] I. R. R. Barani, K.-L. Wong, Y.-X. Zhang, and W.-Y. Li, "Low-profile wideband conjoined open-slot antennas fed by grounded coplanar waveguides for 4 × 4 5G MIMO operation," *IEEE Trans. Antennas Propag.*, vol. 68, no. 4, pp. 2646–2657, Apr. 2020.

[4] K.-L. Wong, C.-J. Chen, and W.-Y. Li, "Integrated four low-profile shorted patch dual-band WLAN MIMO antennas for mobile device applications," *IEEE Trans. Antennas Propag.*, vol. 69, no. 6, pp. 3566–3571, Jun. 2021.

[5] D. Manteuffel and R. Martens, "Compact multimode multielement antenna for indoor UWB massive MIMO," *IEEE Trans. Antennas Propag.*, vol. 64, no. 7, pp. 2689–2697, Jul. 2016.

[6] N. L. Johannsen, N. Peitzmeier, P. A. Hoeher, and D. Manteuffel, "On the feasibility of multi-mode antennas in UWB and IoT applications below 10 GHz," *IEEE Commun. Mag.*, vol. 58, no. 3, pp. 69–75, Mar. 2020.

[7] K.-L. Wong, J.-Z. Chen, and W.-Y. Li, "Four-port wideband annular-ring patch antenna generating four decoupled waves for 5G multi-input–multi-output access points," *IEEE Trans. Antennas Propag.*, vol. 69, no. 5, pp. 2946–2951, May 2021.

[8] J.-S. Row and S.-H. Chen, "Wideband monopolar square-ring patch antenna," *IEEE Trans. Antennas Propag.*, vol. 54, no. 4, pp. 1335–1339, Apr. 2006.

[9] K.-L. Wong, H.-J. Chang, J.-Z. Chen, and K.-Y. Wang, "Three wideband monopolar patch antennas in a Y-shape structure for 5G multi-input–multi-output access points," *IEEE Antennas Wireless Propag. Lett.*, vol. 19, no. 3, pp. 393–397, Mar. 2020.

[10] Y. T. Lo, D. Solomon, and W. Richards, "Theory and experiment on microstrip antennas," *IEEE Trans. Antennas Propag.*, vol. AP-27, no. 2, pp. 137–145, Mar. 1979.

[11] K. F. Lee, Y. X. Guo, J. A. Hawkins, R. Chair, and K. M. Luk, "Theory and experiment on microstrip patch antennas with shorting walls," *IEE Proc.–Microw., Antennas Propag.*, vol. 147, no. 6, pp. 521–525, Dec. 2000.

[12] K.-L. Wong, C.-M. Chou, Y.-J. Yang, and K.-Y. Wang, "Multipolarized wideband circular patch antenna for fifth-generation multi-input–multi-output access-point application," *IEEE Antennas Wireless Propag. Lett.*, vol. 18, no. 10, pp. 2184–2188, Oct. 2019.

[13] (2019). *ANSYS HFSS*. Accessed: Jun. 4, 2019. [Online]. Available: https://www. ansys.com/en/products/electronics/ansys-hfss

[14] M. S. Sharawi, "Printed multi-band MIMO antenna systems and their performance metrics," *IEEE Antennas Propag. Mag.*, vol. 55, no. 5, pp. 218–232, Oct. 2013.

[15] M. Manteghi and Y. Rahmat-Samii, "Multiport characteristics of a wideband cavity backed annular patch antenna for multipolarization operations," *IEEE Trans. Antennas Propag.*, vol. 53, no. 1, pp. 466–474, Jan. 2005.

[16] Y.-L. Ban, C. Li, C.-Y.-D. Sim, G. Wu, and K.-L. Wong, "4G/5G multiple antennas for future multi-mode smartphone applications," *IEEE Access*, vol. 4, pp. 2981–2988, 2016.

KIN-LU WONG (Fellow, IEEE) received the B.S. degree in electrical engineering from the National Taiwan University, Taipei, Taiwan, in 1981, and the M.S. and Ph.D. degrees in electrical engineering from Texas Tech University, Lubbock, TX, USA, in 1984 and 1986, respectively.

From 1986 to 1987, he was a Visiting Scientist with the Max-Planck-Institute for Plasma Physics, Munich, Germany. Since 1987, he has been with the Electrical Engineering Department, National Sun Yat-sen University (NSYSU), Kaohsiung, Taiwan, where he became a Professor, in 1991. From 1998 to 1999, he was a Visiting Scholar with the ElectroScience Laboratory, The Ohio State University, Columbus, OH, USA. He was elected as a Sun Yat-sen Chair Professor at NSYSU, in 2005, a Distinguished Chair Professor at NSYSU, in 2017, and a National Chair Professor at the Ministry of Education of Taiwan, in 2016. He also served as the Chairperson for the Electrical Engineering Department, from 1994 to 1997, the Vice President for Research Affairs, from 2005 to 2007, and the Senior Vice President for NSYSU, from 2007 to 2012. He is currently a National Chair Professor with the Ministry of Education, a Distinguished Researcher with the Ministry of Science and Technology, a Distinguished Chair Professor with the National Sun Yat-sen University, a Thomson Reuters Highly Cited Researcher, and an Elsevier Most Cited Researcher. He has authored more than 580 refereed journal articles and 300 conference papers and has personally supervised 57 graduated Ph.D. students. He holds over 300 patents, including over 100 U.S. patents. He is the author of *Design of Nonplanar Microstrip Antennas and Transmission Lines* (Wiley, 1999), *Compact and Broadband Microstrip Antennas* (Wiley, 2002), and *Planar Antennas for Wireless Communications* (Wiley, 2003). His published articles have been cited over 33,000 times with an H-index of 86 in Google Scholar. He was elected as a Thomson Reuters Highly Cited Researcher, in 2014 and 2015, and an Elsevier Most Cited Researcher, in 2015. In 2008, the research achievements on handheld device antennas of NSYSU Antenna Laboratory led by him was selected to be top 50 scientific achievements of the Taiwan Ministry of Science and Technology, in past 50 years (1959–2009).

Dr. Wong also served as an IEEE AP-S AdCom Member, an IEEE AP-S Transactions Track Editor/Associate Editor, an AP-S Transactions Paper Awards Committee Member, and an AP-S Field Awards Committee Member. He has been an international steering committee member for many international conferences. He received the Outstanding Research Award from the Taiwan National Science Council, in 1995, 2000, and 2002. He also received the Outstanding Electrical Engineering Professor Award from the Institute of Electrical Engineers of Taiwan, in 2003, and the Outstanding Engineering Professor Award from the Institute of Engineers of Taiwan, in 2004. He and his graduate students have been awarded the Best Paper Award (APMC Prize) at the 2008 APMC and the Best Student Paper Award/Young Scientist Award at the 2007 ISAP, 2008 APMC, 2009 ISAP, 2010 ISAP, 2012 ISAP, and 2016 ISAP. His graduate students also won the First Prize of the 2007 and 2009 Taiwan National Mobile Handset Antenna Design Competition. He was a recipient of the 2010 Outstanding Research Award of Pan Wen Yuan Foundation and selected as top 100 Honor of Taiwan by Global Views Monthly, in August 2010, for his contribution in mobile antenna researches. He was also a recipient of the Academic Award from the Taiwan Ministry of Education, in 2012, and the Outstanding Distinguished Researcher Award from the Taiwan Ministry of Science and Technology, in 2013. He was awarded the Best Associate Editor for the IEEE TRANSACTIONS ON ANTENNAS AND PROPAGATION, in 2015 and 2016. He was also a PE7 Panel Member of the 2015, 2017, and 2019 European Research Council Advanced Grant Panel, and a Chief Consultant of the Institute of Antenna Engineers of Taiwan. He also served as the Chair of the Judge Panel for the 2014–2021 National Communication Antenna Design Competition organized by the Taiwan Ministry of Economics. He served as the General Chair for 2012 APMC, 2014 ISAP, and 2016 APCAP, Kaohsiung.

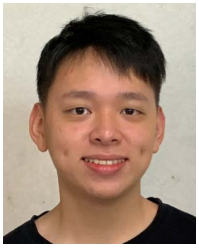

XIAN-QI YE (Student Member, IEEE) received the B.S. degree in electrical engineering from the Southern Taiwan University of Science and Technology, Tainan, Taiwan, in 2020. He is currently pursuing the M.S. degree with the National Sun Yat-sen University, Kaohsiung, Taiwan. His main research interest includes MIMO antennas for 5G access-point applications.

WEI-YU LI (Member, IEEE) was born in Taipei, Taiwan, in 1981. He received the B.S. degree in electrical engineering from Feng Chia University, Taichung, Taiwan, in 2004, and the M.S. and Ph.D. degrees in electrical engineering from the National Sun Yat-sen University (NSYSU), Kaohsiung, Taiwan, in 2006 and 2009, respectively.

After graduated from NSYSU, in 2009, he was with the Information and Communication Research Laboratories (ICL), Industrial Technology Research Institute (ITRI), Hsinchu, Taiwan, participating and leading advanced research for development of emerging wireless antenna technologies. From April to October 2012, he was an Exchange Guest Researcher with the National Institute of Information and Communications Technology (NICT), Tokyo, Japan. He is currently the Deputy Technology Manager with ITRI. He has authored and coauthored 30 refereed journal articles and 40 conference papers. He holds over 70 patents, including U.S., Taiwan, China, and EU patents. His published articles have been cited over 1,277 times with an H-index of 20 in Google Scholar.

Dr. Li received the Young Scientist Award at 2007 ISAP and the Best Paper Award (APMC Prize) at 2008 APMC. He has been principal investigator or co-principal investigator of many research projects in ITRI and has received numerous recognitions, including the First Prize of the Outstanding Research Award of ITRI, in 2010, the Solar Industrial Award (SIA) of Europe, in 2011, the Outstanding Innovation Award of ITRI, in 2013, the Second Prize of the Outstanding Research Award of ITRI, in 2014, the 2015 Research and Development 100 Award Finalist of the U.S., the Outstanding Innovation Award of ITRI, in 2017, the First Prize of the Outstanding Industrialization Award of ITRI, in 2017, the Second Prize of the Outstanding Industrialization Award of ITRI, in 2020, and the Third Prize of the Outstanding Industrialization Award of ITRI, in 2021. He also received the Outstanding Lecturer Award of ITRI, in 2013, and the International Paper Award of ICL of ITRI, in 2020. He has been selected as an International Steering Committee Member of 2019 ISAP, 2020 ISAP, 2021 ISAP, and has been selected as the Chair of IEEE AP-S Tainan Chapter, in 2021 and 2022. He served as an AdCom Member for the Institute of Antenna Engineers of Taiwan, in 2014, 2015, and 2018–2021. He also served as one Member of the Judge Panel for the 2014 to 2021 National Terminal Antenna Design Competition organized by the Taiwan Ministry of Economics.